Structure Of The Neutron-Rich Cr Isotopes: Inadequacy Of The *fp* Model Space And Onset Of Deformation

S. J. Freeman[a,b], R. V. F. Janssens[b], B. A. Brown[c], I. V. Calderin[d], M. P. Carpenter[b], P. Chowdhury[b,e], A. N. Deacon[a], S. M. Fischer[f], N. J. Hammond[b], M. Honma[g], T. Lauritsen[b], C. J. Lister[b], T. L. Khoo[b], G. Mukherjee[b,e], D. Seweryniak[b], J. F. Smith[a], S. L. Tabor[d], B. J. Varley[a], M. Whitehead[a], and S. Zhu[b,h]

[a]*Department of Physics and Astronomy, University of Manchester, Manchester M13 9PL, UK*
[b]*Physics Division, Argonne National Laboratory, Argonne, IL 60439, USA*
[c]*National Superconducting Cyclotron Laboratory, Michigan State University, East Lansing, MI 48824, USA*
[d]*Department of Physics, Florida State University, Tallahassee, FL 32306, USA*
[e]*Department of Physics, University of Massachusetts Lowell, Lowell, MA 01854, USA*
[f]*DePaul University, Chicago, IL 60604, USA*
[g]*University of Aizu, Fukushima 965-8580, Japan*
[h]*University of Notre Dame, South Bend, IN 46556, USA*

Abstract. The low-lying levels in ^{59,60}Cr have been populated with ^{13,14}C(^{48}Ca, 2*p*) reactions using a beam energy of 130 MeV. Prompt electromagnetic radiation was detected using the Gammasphere array, in coincidence with the detection of recoiling ions performed with the Fragment Mass Analyzer and a gas-filled ion chamber. The residues of interest were selected and identified on the basis of charge-to-mass ratio, energy-loss and time-of-flight measurements. These methods have isolated γ rays from the *2p* evaporation channel for the first time. The low-lying structure of ^{59}Cr is clearly inconsistent with the results of shell-model calculations within the full *fp* shell model and requires the inclusion of the $g_{9/2}$ orbital. The sequence of states can be understood within the Nilsson model assuming a moderate oblate ground-state deformation. Preliminary results for ^{60}Cr are discussed in terms of the development of deformation in the region. None of the low-lying structures observed so far exhibit a clear indication for a well-developed oblate shape.

INTRODUCTION

The region bound by N = 28–40 and Z = 20–28 is of particular interest to the development of the shell model in neutron-rich systems. Extension of the shell-model approach to such regions, far from stability, requires novel model spaces and the effective interactions within these new spaces must be determined. The full $\pi f_{7/2}\nu fp$ space is small enough for large-scale calculations to be attempted and, recently, new effective interactions have been developed [1]. These calculations have been successful in describing the N = 32 subshell closure and its gradual demise with increasing Z above Ca [2,3], and predict a similar N = 34 subshell gap between the $\nu f_{5/2}$ and $\nu p_{1/2}$ orbitals. The N = 34 gap has not been substantiated in recent studies of Ti isotopes [4]. The success of this particular model space depends sensitively on the effect of the gap between neutron orbitals at N = 40, an interesting issue considering that even the doubly-magicity of ^{68}Ni has attracted some controversy recently [5]. The strength of such a shell closure depends not only on the energetic separation of orbitals, but also on the ease with which excitations can be generated across it. A large N = 40 gap effectively isolates the low-lying structure from the neutron $g_{9/2}$ orbital, whereas a weak shell closure facilitates excitations involving it. Such excitations would have clear structural implications as this orbital has considerable deformation-driving effects. The presence of a weak N = 40 subshell closure would present challenges for the shell model in terms of the necessity to enlarge the space to include the $\nu g_{9/2}$ orbital and to develop an effective interaction within the enlarged space.

CP764, *Nuclei at the Limits,* edited by D. Seweryniak and T. L. Khoo

The chromium isotopes lie in the middle of the $\pi f_{7/2}$ shell and would be naively expected to experience the greatest collective effects in the region. In fact, recent measurements following the β decay of ^{60,62}V fragmentation products [6] have indicated the presence of γ-ray transitions with energies of 646 and 446 keV in ^{60,62}Cr. These data have led the authors to speculate that these isotopes may have substantial oblate deformation with shape parameters, $\beta_2 \approx 0.3$. The present work was undertaken to extend this basic information in order to substantiate these speculations.

The production of neutron-rich isotopes still presents a major challenge. Projectile fragmentation yields neutron-rich fragments and γ rays following β decay can be studied, but the production yields generally restrict these measurements to singles events. Deep-inelastic and multi-nucleon transfer reactions can produce neutron-rich products and some pioneering measurements [7] have been made with high-fold γ-ray data on nuclei where at least one transition is known from other work. Experimental facilities to perform γ-ray measurements in coincidence with isotopic identification of quasi-elastic reaction products are currently being developed [8]. In this work a different approach is taken using fusion-evaporation reactions. The most neutron-rich stable targets and projectiles have been used to produce the most exotic compound nucleus possible. Most of the subsequent evaporation is via neutron emission taking the system back towards stability, but rare two-proton evaporation actually increases the proton deficiency of the residues. Evaporation models indicate that the strongest evaporation channels in the reactions used here are the 3*n* and 4*n* channels with cross sections of several hundred mb, in contrast to the cross sections for multiple proton emission which are at the level of a few μb. Very selective techniques are, therefore, necessary to extract events from such weak channels.

EXPERIMENTAL DETAILS AND SELECTION/IDENTIFICATION TECHNIQUES

An ECR ion source was used to generate $^{48}Ca^{11+}$ ion beams which were subsequently accelerated to energies of 130 MeV using the ATLAS Superconducting Linear Accelerator at Argonne National Laboratory. These were used to bombard enriched ^{13,14}C targets, with approximate thicknesses of 100μgcm^{-2}, in two separate experiments. In both cases, the isotopic enrichment was at a level of about 90%, the main contaminant being ^{12}C. Prompt γ rays were detected using the Gammasphere array [9]. Ions recoiling from the target position were separated from primary beam particles and dispersed along a focal plane according to their charge-to-mass (*A/q*) ratio using the Fragment Mass Analyzer (FMA) [10], which was tuned to transport ions with charge state 17+ and mass 59/60 to the middle of the focal plane. In such inverse reactions, the *A/q* for certain beam charge states is similar to that of the beam, so slits were used to further reduce the effects of scattered beam. Higher energy particles were blocked by introducing a slit at the exit of the first electric dipole of the FMA and slits were also introduced to mask unwanted regions of the focal plane. A parallel-grid avalanche counter (PGAC) at the focal plane was used to measure the horizontal and vertical positions of the recoils, behind which a segmented ion chamber recorded their rate of energy loss. The data acquisition was triggered by an event corresponding to the arrival of an ion at the focal plane in coincidence with the detection of at least one γ ray in Gammasphere. Data were recorded with the ^{13}C target for a total of 58 hours and with the radioactive ^{14}C target for 128 hours, both with beam currents of approximately 5 pnA.

The isotopic selection techniques used will be discussed with the ^{14}C(^{48}Ca, 2*p*)^{60}Cr reaction as an example; similar methods were used to isolate ^{59}Cr in the reaction on the ^{13}C target and are described elsewhere [11]. Tagging using a recoil-mass spectrometer, which is dispersive in terms of *A/q,* can suffer from so-called charge-state ambiguities, where ions with different mass and charge appear at the same position on the focal plane. For example, $^{60}Cr^{17+}$ ions have an *A/q* ratio of 3.529 which is close to that of $^{56}Cr^{16+}$ ions, 3.500. The combination of the total ion energy, *E,* and the time of flight through the FMA, *T*, in the form ET^2 is proportional to the mass of the ion and can be used to help resolve these ambiguities. This is shown in Fig. 1 (a), where the total energy deposited in the ion chamber is used as an estimate of *E* and the time of flight is deduced from the time of the PGAC anode signal relative to an accelerator radiofrequency signal. The resolution in such a measurement, whilst being poor, is sufficient to separate the *A/q*=60/17 ions from the *A/q*=56/16 group. The atomic number of the recoiling ions is easily deduced from the energy-loss characteristics of the ions in the gas-filled ion chamber, as illustrated in Fig. 1 (b), where the energy deposited in the front segment of the chamber, ΔE, is plotted against the sum of the ion chamber signals, *E*. The Cr band in this plot has two distinct lobes which occur as the Cr yield is dominated by the reaction, ^{14}C(^{48}Ca, $\alpha 2n$); the acceptance of the FMA restricts the α-particle evaporation to tight cones, up and down the beam direction, leading to high- and low-energy ^{56}Cr ion groups. Similar effects occur in the Ti group which is produced predominantly by 2α evaporation.

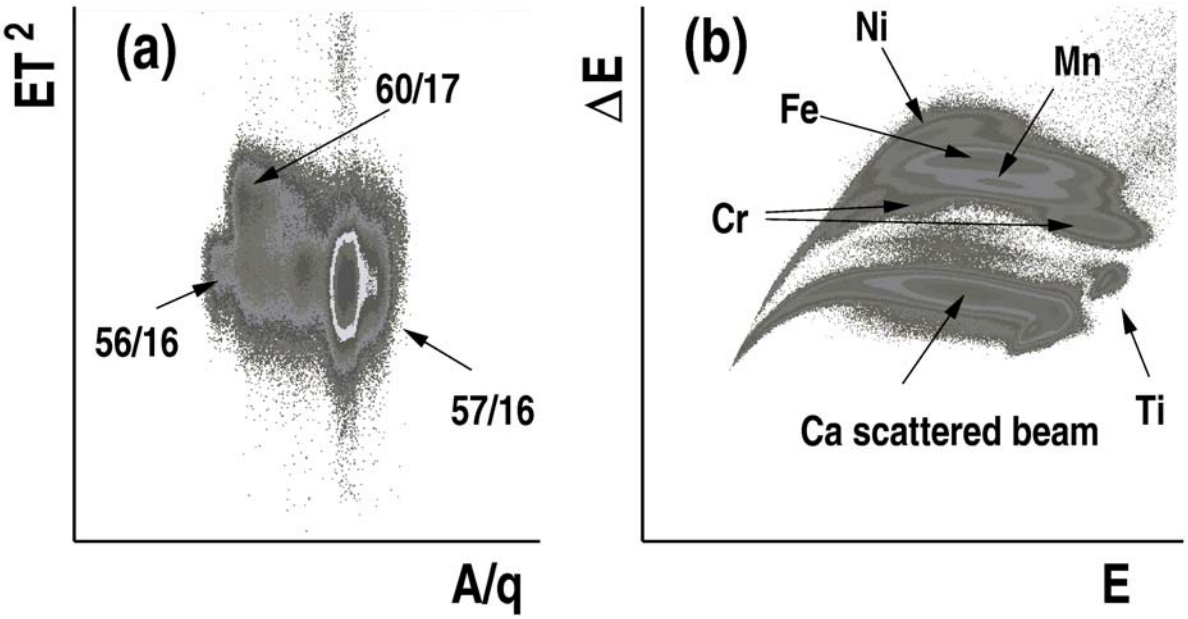

FIGURE 1. Two-dimensional plots for ion identification: (a) ET^2 versus charge-to-mass ratio, A/q, of ions. Various ion groups are labeled by A/q. (b) Energy loss versus total energy in the ionization chamber (see text for details). Various elemental ion groups are labeled. All axes are in arbitrary units.

Polygonal gates on the groups in Fig. 1 are used to select events corresponding to A/q=60/17 and Z=24 ions; coincident γ-ray transitions are illustrated in Fig. 2. Panel (a) shows the raw spectrum with these gates applied. It is clear that the tail of the considerably more intense A/q=56/16 ion group leaks into this gate. The peaks arising from this channel have a noticeably larger width arising from a larger spread in recoil velocities associated with α-particle evaporation. Other lines are present which, without the ET^2 selection, would be obscured by the A/q=56/16 transitions and associated background. Figure 2 (b) shows the spectrum gated on the tail of the A/q=56/16 group, away from the A=60 peak, clearly identifying the leak-through peaks. Figure 2 (c) shows a normalized subtraction of these two spectra; peaks in this spectrum are, therefore, assigned as transitions in ^{60}Cr.

Further evidence for the mutual association of these transitions can be obtained through analysis of $\gamma\gamma$ coincidences. Figure 3 shows some coincident γ-ray energy spectra from the A=60, Z=24 data. Figure 3 (a) illustrates a spectrum gated by a transition energy of 645 keV. The data is scarce; the average number of counts per channel is considerably less than one count and so peaks consisting of only a small number of counts are significant in the spectrum. Of the candidate transitions shown in Fig. 2, all but the 1031-keV transition are present in the gated spectrum. The 1031-keV transition is considerably weaker than the others, and its width suggests that it could be a doublet [see Fig. 2(c)]. As a result, the non-appearance of such a low-intensity transition may in itself not be significant when dealing with this overall level of statistics. In addition to the original candidate transitions, there is also another line at an energy of 1175 keV. This has roughly half the intensity of the 986-keV transition and is unresolved from a strong transition in the contaminating nucleus, ^{56}Cr, which accounts for the lack of an obvious transition with this energy in Fig. 2 (c). Good spectra gated at energies of 819 and 986 keV were obtained [Fig. 3 (b) and (c)], but other lines were either too weak or too contaminated. Using these data, the level scheme presented in Fig. 4 was constructed, where spins were assigned on the assumption of a zero-spin ground state and yrast feeding.

Very similar techniques were used to determine transitions in ^{59}Cr and the deduced level scheme is shown in Fig. 4. The spin assignments were made by combining previous information on the β decay of the ground state with new information obtained in the current experiments on ^{59}Mn, and in addition to some model-dependent arguments about non-observation of cross-over transitions in the level scheme [11].

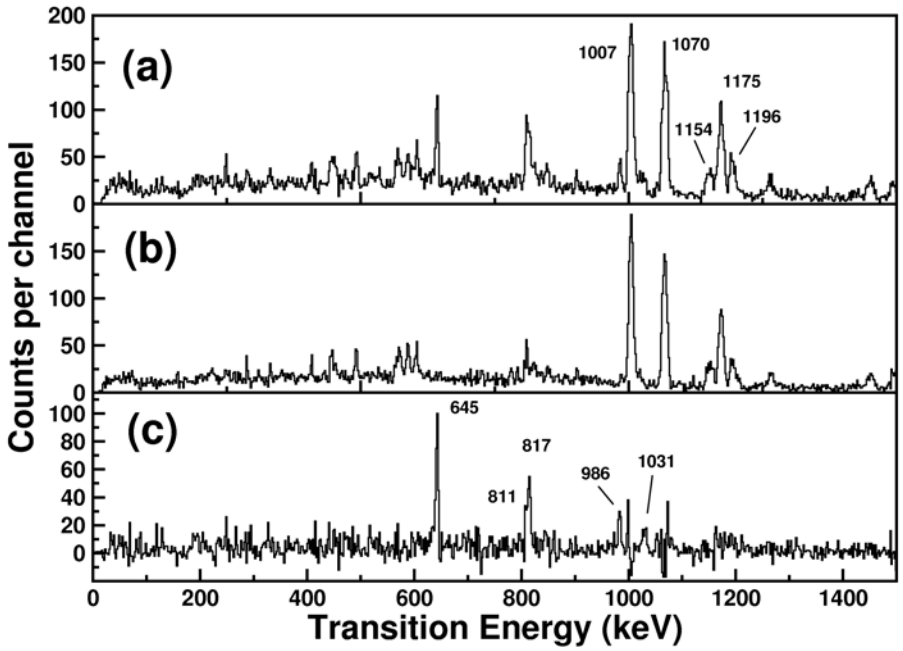

FIGURE 2. Singles γ-ray spectra with various channel selection cuts applied: (a) is gated by A/q=60/17 and Z=24. Transitions previously known in ^{56}Cr [13] are labeled by the transition energy quoted to the nearest keV. (b) is gated by A/q=56/16 and Z=24, and (c) is the normalized subtraction of (b) from (a). (See text for details).

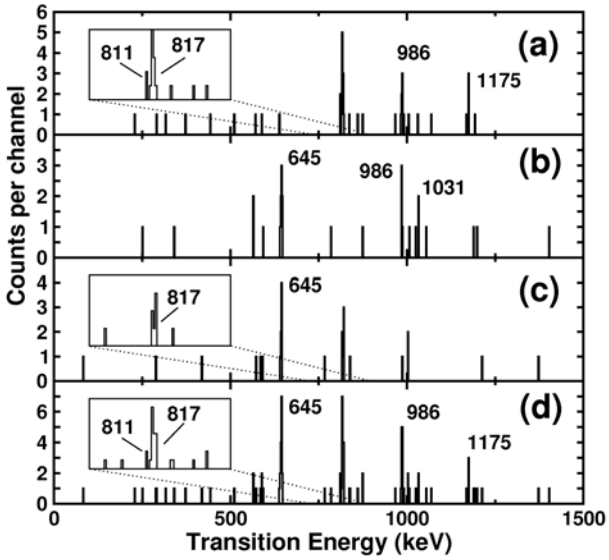

FIGURE 3. Coincident γ-ray energy spectra for A/q=60/17 and Z=24 data. The spectra gated by γ-ray energies of (a) 645 keV, (b) 819 keV (the gate is slightly higher than the actual transition energy to avoid contaminant peaks), and (c) 986 keV. Spectrum (d) shows the sum of these gates. The insets in the spectra show the region between 750 and 900 keV. Peaks are labeled by their transition energy to the nearest keV.

RESULTS AND CONCLUSIONS

The deduced level schemes are shown in Figs. 4 (a) and (b). These results represent significant extensions of previous work, which had established only a 646-keV transition in ^{60}Cr [6] and two prompt transitions at 103 and 207 keV in ^{59}Cr [12]. No evidence was presented for the ordering of these transitions in ^{59}Cr.

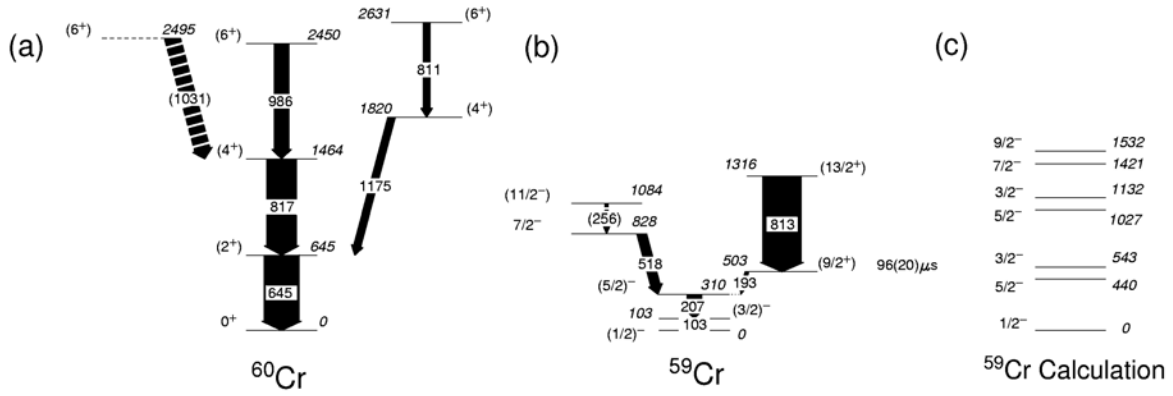

FIGURE 4. Energy levels in neutron-rich chromium isotopes. (a) The ^{60}Cr level scheme derived from the current work. (b) The ^{59}Cr level scheme (see Ref. [11] for details). (c) Energy levels of ^{59}Cr from a shell-model calculation within the full *fp*-shell basis using the GXPF1 interaction [1]. Note that the intensity of the 1031-keV transition is the full peak area shown in Fig. 2 (c), but it is likely that this is a doublet.

The low-lying structure of ^{59}Cr should reflect single-neutron excitations within the $1f_{5/2}$, $2p_{1/2}$, and $2p_{3/2}$ orbitals, along with $1g_{9/2}$ depending on the strength of the N=40 closure. β decay feeds the $5/2^-$ state at 310 keV and possibly the $3/2^-$ state at 103 keV [12], suggesting an $f_{5/2}$ parentage for at least the $5/2^-$ state via allowed $\pi f_{7/2} \rightarrow \nu f_{5/2}$ decays. Calculations, performed within the full *fp*-shell basis using the GXFP1 interaction [1], are shown in Fig. 4(c). Although the spin and parity of the ground state are reproduced, comparison with the experimental level scheme reveals a failure to provide a description of the low-lying states; the experimental levels are ordered differently and are compressed compared with the calculation. Furthermore the low-lying $9/2^+$ state is very obviously outside of the fp-model space. Observation of this state at such a low excitation energy, as well as clearly demonstrating the necessity of including the $1g_{9/2}$ orbital in the calculation, also suggests the presence of deformation. For small oblate deformations, within a deformed Woods-Saxon calculation [11], the $9/2^+$ state from this orbital falls dramatically in energy towards the Fermi surface to energies consistent with the experimental observation. In addition, a deformation of this size also reproduces the ground-state spin which may indicate that the ground state is also non-spherical. Both of these features are not reproduced for prolate shapes. The other low-lying excited states also appear consistent with a moderate oblate ground-state deformation (see [11] for details). Such inferences from simple level sequences provide a qualitative insight, but reality is likely to be more complex. The presence of gaps at N=34 for *both* oblate and prolate shapes suggests that shape coexistence may arise, or that levels with admixtures of oblate and prolate states may form the basis of many low-lying states. There is an interesting parallel here between the A=60 and A=80 regions; the neutron Fermi surface has a similar position in terms of single-particle orbitals to that for both types of nucleons in the A=80 region, where oblate and prolate shape coexistence is well established. Although the strong cooperative effects between protons and neutrons in the same orbitals is lacking in the A=60 region, similar phenomena may occur.

In passing, it is interesting to note the similarity in energy of the 813-keV transition feeding the $9/2^+$ state to that of the $2^+ \rightarrow 0^+$ transition in ^{58}Cr at 880 keV [13]. This may be another example of the same weak coupling between the odd neutron and the core that has been observed in other less neutron-rich systems.

The structure of ^{60}Cr also appears to cast doubt on interpretations involving well-developed oblate deformation. Whilst arguments on the basis of the first 2^+ energy and simple systematics presented in Ref. [6] might suggest a large oblate shape, the low-lying structure of ^{60}Cr does not have characteristic features that would be associated with a well-developed stable oblate configuration. The $E(4^+)/E(2^+)$ ratio, for example, is only 2.27. If oblate deformation is present, the observed structure suggests significant mixing with other shapes. Any minima in the total energy surface are likely to be rather diffuse. The presence of a second low-lying 4^+ state might lead to the speculation that

this is, in fact, the next oblate state in the sequence after the first-excited state. The $E(4^+)/E(2^+)$ ratio for this combination, 2.82, does approach that expected for a rotor. Given the tentative nature of the spin assignments, and the current lack of any corroborating calculations, such arguments remain speculative.

The cross sections inferred from the observed yields for the ^{13,14}C(^{48}Ca, 2*p*) reactions are approximately 10 and 5 μb respectively, assuming an FMA transmission of 5% in each case. This is the first time that such multiple charged-particle evaporation channels have been isolated in the neutron-rich *fp* shell and these channels have proved to be a viable route with which to perform spectroscopy. These experiments have benefited from the availability of neutron-rich targets and projectiles to the extent that they have become competitive with other mechanisms for the production of neutron-rich nuclei. The information gathered here is clearly more extensive than previous studies of fragmentation products. Deep-inelastic reactions can penetrate into this region, but thick-target experiments have suffered from the lack of isotopic identification, unless at least one γ-ray transition is already known. Some of the transitions observed here can be seen in reactions of ^{48}Ca on ^{238}U at beam energies of ~25% above the fusion barrier, given the isotopic identification of transitions gained in the current work [14]. There are clearly opportunities to use the 2*p* evaporation channel in the study of other neutron-rich systems. The extension of these identification methods to the 3*p* channel requires increased beam energy. The use of the FMA in such cases would require degradation of the recoil energy prior to entering the separator. Given the particular issues with scattered beam in these inverse reactions, whilst not being impossible, this would require development.

In summary, two-proton evaporation from neutron-rich *fp*-shell compound nuclei has been observed for the first time in the fusion of ^{48}Ca beams with ^{13,14}C targets. Recoiling evaporation residues have been identified using recoil-mass and energy-loss techniques and these measurements have been used to tag coincident prompt γ-ray emission. These data have been used to establish the low-lying structure of ^{59,60}Cr. The low-lying levels of ^{59}Cr are clearly at variance to full *fp* shell-model calculations and the influence of the $\nu g_{9/2}$ orbital is evident at low excitation energy. The observed sequence of states appears to be consistent with the presence of a moderately deformed oblate ground-state shape. The sequence of states in the neighboring even-even nucleus, ^{60}Cr, suggests that such deformation is not well developed. Calculations of the total-potential-energy surfaces around mass 60 are currently being undertaken to set these findings within a theoretical context.

ACKNOWLEDGMENTS

This work was supported by the UK EPSRC, the U.S. National Science Foundation under Grant No.s PHY-0244453 and PHY-0139950, and the U.S. Department of Energy, Office of Nuclear Physics, under contract W-31-109-ENG-38 and DE-FG02-94ER40848. The authors would like to thank the group at University of Birmingham for the use of their ^{14}C target.

REFERENCES

1. M. Honma, T. Otsuka, B. A. Brown, and T. Mizusaki, Phys. Rev. C **65**, 061301 (2002).
2. J. I. Prisciandaro *et al.,* Phys. Lett. **B510**, 17 (2001).
2. R. V. F. Janssens *et al.,* Phys. Lett. **B546**, 55 (2002).
3. S. N. Liddick *et al.,* Phys. Rev. Lett. **92**, 072502 (2004) and D.-C Dinca, proceedings of this meeting.
5. K. Langanke, J. Terasaki, F. Nowacki, D. J. Dean, and W. Nazarewicz, Phys. Rev. C **67**, 044314 (2003).
6. O. Sorlin *et al.*, Eur. J. Phys. **16**, 55 (2003).
7. For example, W. Królas *et al.*, Nucl. Phys. **A724**, 289 (2003).
8. A. Gadea *et al.,* Eur. Phys. J. A **20** (2004) 193.
9. I. Y. Lee, Nucl. Phys. **A520**, 641c (1990).
10. C. N. Davids *et al.,* Nucl. Instrum. Methods Phys. Res. **B70**, 358 (1992).
11. S. J. Freeman *et al.*, Phys. Rev. C **69**, 064301 (2004) and C **70**, 029901 (2004).
12. O. Sorlin *et al.*, Nucl. Phys. **A669**, 351 (2000).
13. P. F. Mantica *et al.*, Phys. Rev. C **67**, 014311 (2003).
14. S. Zhu and R. V. F. Janssens, Private communication (2004).